Proceedings of Ninth World Conference on Earthquake Engineering
August 2-9, 1988, Tokyo-Kyoto, JAPAN (Vol.III)

5-2-9

NON-LINEAR RESPONSE ANALYSIS OF SOIL-STRUCTURE INTERACTION SYSTEMS USING KINEMATIC CAP MODEL FOR SOIL

Yasuo Tanaka[1], Mamoru Mizutani[2], Harumi Yashiro[3],
Hidenobu Araki[4], and Takahiro Abe[5]

[1]Professor, Dept. of Architecture, Waseda University, Tokyo, Japan
[2]Research Engineer, Tokyo Electric Power Services Co.,Ltd., Tokyo Japan
[3]Research Associate, Dept of Architecture, Waseda University, Tokyo Japan
[4]Engineer, Kawasaki Steel Co.,Ltd, Tokyo, Japan
[5]Structural Engineer, Takenaka Komuten Co.Ltd, Osaka, Japan

SUMMARY

In the dynamic response analysis of soil-structure systems, two types of non-linearity, that is, matarial non-linearity of the soil and geometrical non-linearity such as the separation of the structure from the soil and the sliding on the soil are taken into consideration.

The soil-structure interaction systems are expressed as plane strain models and structures are assumed to be elastic in this study. The soil-structure interaction systems are subjected to harmonic waves and are analysed by using finite element method. The soil is represented by the non-linear kinematic cap model based on classic theory of elastoplasticity. To express separation and sliding between the structure and the soil, interface elements are used.

INTRODUCTION

Under intense earthquake, it is pointed out that various non-linearities work on soil-structure systems and in the dynamic response analyses of soil-structure systems, taking non-linearities such as material non-linearity of the soil and geometrical non-linearity between the structure and the soil into account is one of the important subjects.

In this study, the dynamic finite element response analysis for simple harmonic excitation is performed considering two types of non-linearity which are material non-linearity for the soil and geometrical non-linearity such as debonding, sliding and rebonding at the interface between the soil and the structure and the effect of these non-linearities on the soil-structure systems is investigated.

The kinematic cap model based on the classic theory of elastoplasticity which was used by D.K.Vaughan (Ref.1) is used as a model representing material non-linearity for the soil. This model can represent explicitly material non-linearity for the soil such as volumetric compaction (negative dilatancy), strain-hardening property under shear loading, volumetric dilatation (positive dilatancy) and kinematic hardening property under shear.

To represent geometrical non-linearity such as debonding, sliding and rebonding, the interface continuum elements for which material non-linearity is considered also are put between the structure and the soil.

Four types of models are considered for calculation. They are the elastic soil model (model EL), the model with material non-linearity of soil (model PL), the model with geometrical non-linearity at the interface (model GE) and the model with material non-linearity of soil and geometrical non-linearity of interface (model GP).

Comparing the results for these models, the response behaviors of soil-structure systems for simple harmonic excitation are discussed.

ANALYTICAL MODEL

The analytical model is shown in Fig.1. This model is dealt analytically as plane-strain problem. The surface layer soil and the backfill soil are considered. The structure is a monolithic concrete block. Rigid boundary is considered for the bottom boundary of the soil and viscous boundary condition is considered for the side boundaries. The impedance ratio for viscous boundary condition is shown in Table 1.

The kinematic cap model which represents material non-linearity for the soil is shown in Fig.2. This model consists of three surfaces in stress space. These are a revised Drucker-Prager failure surface F_L which is fixed in stress space, a small revised Drucker-Prager yield surface F_1, which expresses kinematic hardening yield surface in F_L, and a strain-hardening cap F_2.

The limit surface F_L bounds the region of stress space within which the yield surfaces F_1 and F_2 may translate.

The yield surface F_1 has the same shape as the limit surface F_L, but bounds a smaller region of stress space and this surface repesents hysteresis under cyclic shear.

The strain-hardening cap F_2 is expressed as a function of a volumetric plastic strain.

If the stress point lies within the strain-hardening cap and the revised Drucker-Prager yield surface, soil behavior is linear elastic. When the stress point is on the strain-hardening cap, by the flow rule plastic strains occur and by deviatoric plastic strain negative volumetric plastic strain occurs. This is volumetric compaction (negative dilatancy). As the increase of stress, the cap expands and translates along hydrostatic pressure axis.

When the stress point is on the revised Drucker-Prager kinematic hardening yield surface, by the flow rule plastic strains occur and by deviatoric plastic strain positive volumetric plastic strain occurs. This is volumetric dilatation (positive dilatancy). As the increase of stress, the cap shrinks.

Table 2 shows the material constants of the kinematic cap model. The other material constants are shown in Table 3.

The interface element is a model which is used to take geometric non-linearity such as debonding, sliding and rebonding into consideration. (See Fig.3) The interface between the structure and the soil is approximated by very thin continuum soil elements. The constitutive material properties of these elements are considered to be the same as those of adjacent soil.

When debonding occurs, to make the effect of the mass of soil to the nodes of the structure as small as possible, the continuum interface element should be thin enough. In this study the ratio B/t' of element thickness t' and element breadth B in Fig.3 is 10.

It is assumed that debonding occurs when the normal stress σ_n equals to 0 (see Fig.4). During debonding, the stiffness of interface element becomes 0 and the transmissions of normal stress and shear stress between the structure and the soil are not performed. If the normal strain ε_n returns to ε_s at the strain of which debonding occurred, it is assumed that rebonding occurs.

It is assumed that sliding occurs when the shear stress becomes yield shear stress τ_y (see Fig.5). The relation between normal stress and yield shear stress is shown in Fig.6. As the normal stress increases, the yield shear stress which causes sliding increases. In the figure, C is cohesive power. During sliding, the same normal stress strain relation as that at normal state is used, but the shear stress is kept at τ_y at which sliding started.

Harmonic waves with the maximum acceleration of 200gal and the periods of 0.5sec and 1.0sec are induced at the fixed boundary.

The soil-structure systems are analysed using finite element method and the

calculation is performed in the time domain for a duration of 5.0sec for which 2000 mesh-time steps are executed by using Wilson's θ method. 8-noded isoparametric elements are used for the structure and the soil elements. 6-noded isoparametric elements are used for the interface elements.

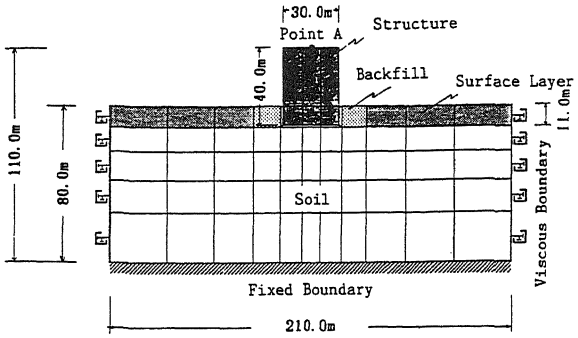

Fig.1 Analytical Model

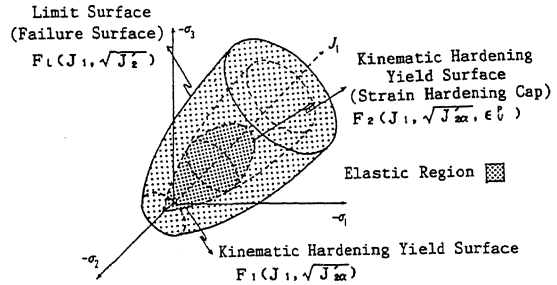

$$F_1(J_1,\sqrt{J_2})=\sqrt{J_2}-A+C\exp(BJ_1)$$
$$F_1(J_1,\sqrt{J_{2\alpha}})=\sqrt{J_{2\alpha}}-(A-N)+C\exp(BJ_1)$$
$$F_2(J_1,\sqrt{J_{2\alpha}},\epsilon_v^p)=(J_1-J_a)^2-(J_a-J_b)^2+R^2J'_{2\alpha}=0$$
$$J_a-J_b=R[(A-N)-C\exp(BJ_a)]$$
$$\epsilon_v^p=W[\exp(DJ_b)-1]$$
$$\dot{\alpha}_{ij}=C_\alpha F_\alpha \dot{e}_{ij}^p$$
$$F_\alpha=\max\left(0,\ 1-\frac{\sigma_{ij}-\alpha_{ij}}{2N[(A-N)-C\exp(BJ_b)]}\right)$$

A,B,C,D,R,W,N,C_α : Material Constants

$J_1=\sigma_{ij}\delta_{ij}=\sigma_{ik}$: First Constant of Stress Tensor σ_{ij}

$J'_2=\frac{1}{2}S_{ij}S_{ij}$: Second Constant of Deviatoric Stress Tensor S_{ij}

$J'_{2\alpha}=\frac{1}{2}(S_{ij}-\alpha_{ij})(S_{ij}-\alpha_{ij})$: Second Constant of Kinematic Deviatoric Stress Tensor $(S_{ij}-\alpha_{ij})$

$\epsilon_v^p=\epsilon_{rs}^p\delta_{rs}\approx\epsilon_{kk}^p$: Volumetric Plastic Strain

$S_{ij}=\sigma_{ij}-\frac{1}{3}J_1\delta_{ij}$: Deviatoric Stress

$\dot{e}_{ij}^p$: Deviatoric Plastic Strain Velocity

α_{ij} : Memory Parameter, $\alpha_{11}+\alpha_{22}+\alpha_{33}=0$

Fig.2 Kinematic Cap Model

Table 1 Impedance Ratio for Viscous Boundary

Impedance Ratio	
a_1	1.0
a_2	1.0

$\sigma_x=a_1\rho V_p u/t$

$\tau_{xy}=a_2\rho V_s v/t$

u : x Direction Displacement
v : y Direction Displacement
ρ : Density
V_s : Shear Wave Velocity
V_p : Compressive Wave Velocity
a_1,a_2 : Impedance Ratio
t : Time

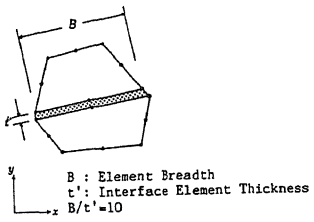

Fig.3 Interface Element

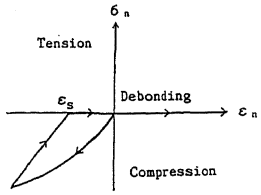

Fig.4 Normal Stress-Strain Relation for Interface Element

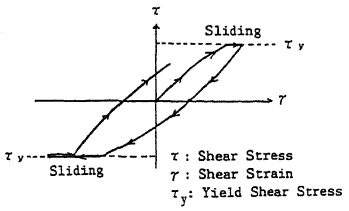

Fig.5 Shear Stress-Strain Relation for Interface Element

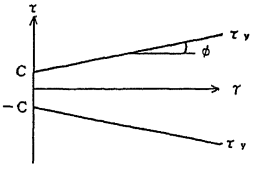

Fig.6 Yield Shear Stress Normal Strain Relation for Interface Element

Table 4 Material Constants for Interface Element

Material Constants	
Tension Intensity σ_t (t/m²)	0
Cohesive Power C (t/m²)	10.0
Inner Friction Angle ϕ (degree)	30

Table 2 Material Constants for Kinematic Cap Model

A (t/m^2)	3.30703×10^2
B (t/m^2)	3.04140×10^{-4}
C (t/m^2)	2.74413×10^2
D (t/m^2)	9.94851×10^{-4}
R	2.5
W	0.066
N (t/m^2)	5.34753×10
C_α (t/m^2)	5.62480×10^3

Table 3 Material Constants

Material Constants	Soil	Surface Layer	Backfill	Structure
Young's Modulus E (t/m^2)	7.03623×10^4	4.00000×10^4	2.00000×10^4	2.10000×10^6
Poisson's Ratio ν	0.25	0.25	0.25	0.17
Unit Mass (t/m^3)	1.80	1.80	1.80	2.40
Volumetric Elastic Coefficient K (t/m^2)	4.69105×10^4	2.66667×10^4	1.33333×10^4	1.05000×10^6
Shear Elastic Coefficient G (t/m^2)	2.81449×10^4	1.60000×10^4	8.00000×10^3	9.00000×10^5
Shear Wave Velocity Vs (m/s)	3.91450×10^2	2.95146×10^2	2.08700×10^2	1.91703×10^3
Compressive Wave Velocity Vp (m/s)	6.78021×10^2	5.11208×10^2	3.61478×10^2	3.03109×10^3

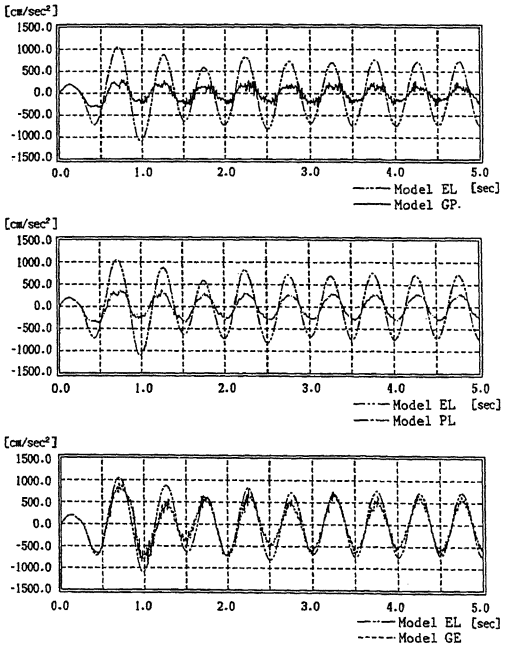

Fig.7 Response Accelaration Time Histories at The Top Point A of The Structure (Period of 0.5sec)

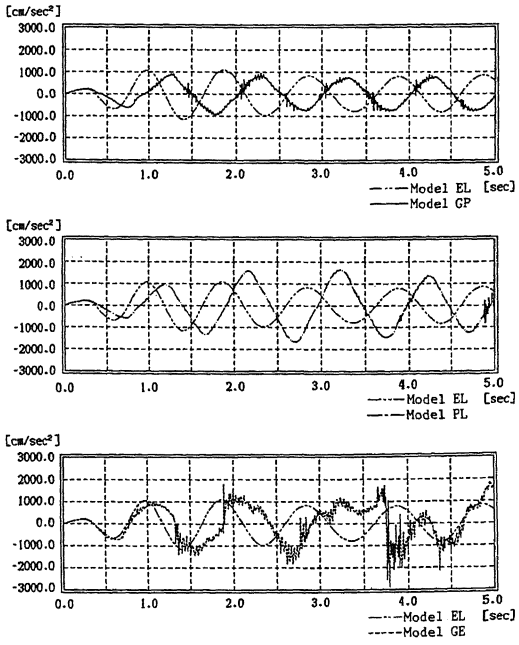

Fig.8 Response Acceleration Time Histories at The Top Point A of The Structure (Period of 1.0sec)

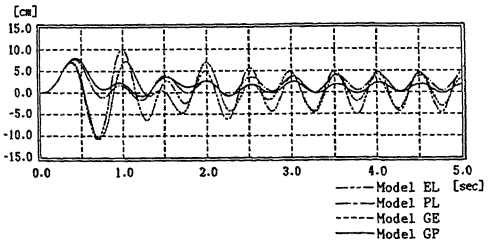

Fig.9 Response Displacement Time Histories at The Top Point A of The Structure (Period of 0.5sec)

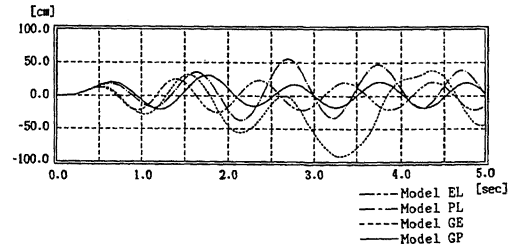

Fig.10 Response Displacement Time Histories at The Top Point A of The Structure (Period of 1.0sec)

DISCUSSION OF RESULTS

RESPONSE TIME HISTORIES The response acceleration at the top point A of the structure for harmonic waves of period 0.5sec and 1.0sec are shown in Figs.7 and 8, respectively.

The responses of four models are different from each other. As seen in Fig.7 the responses of models PL, GE and GP are smaller than those for model EL. But, in Fig.8 the response of model PL is rather large. These phenomena may be the results of soil plastification which will cause the change of general response of the soil-structure systems. From these figures it is seen that the energy damping caused by the material non-linearity for soil and the geometrical non-linearity for interface will depend on frequency.

In Fig.7 response phase lag is not seen, but in Fig.8 response phase lag is seen.

As for the response acceleration high frequency components appear in models PL, GE and GP. This may be the results that material non-linearity for soil and geometrical non-linearity for interface cause high frequency component response. High frequency response is seen clearly in model GE. This will be the results of rebonding at the interface. The responses of model GP are less than those of model GE. This will be the results of interaction of two non-linearities.

The response displacement-time histories at the top A of the structure are shown in Figs.9 and 10.

Comparing the responses for 0.5sec and 1.0sec sine waves, those for latter waves are larger than those for the former waves. Especially the responses of model GE for 1.0sec sine waves are very large. This will be the effect of debonding at the interface.

OVERALL SOIL RESPONSE Figures 11 and 12 show overall soil behavior. It is seen that the soil accelerations around the structure are rather large. It is considered this will be the rebonding effects.

Concerning the overall soil behaviors, it is seen the soil beneath the structure and near the fixed boundary is comparatively stable due to the cap model expansion by the loading from the structure.

The region of shear yielding for model PL is larger than that for model GP. This is because the stresses are overestimated by taking no geometrical non-linearity into account in model PL.

Comparing the behaviors for sine waves of periods of 0.5sec and 1.0sec, the soil plastification processes are different from one another. This shows that the nature of soil plastification depends largely on the periods of input seismic waves.

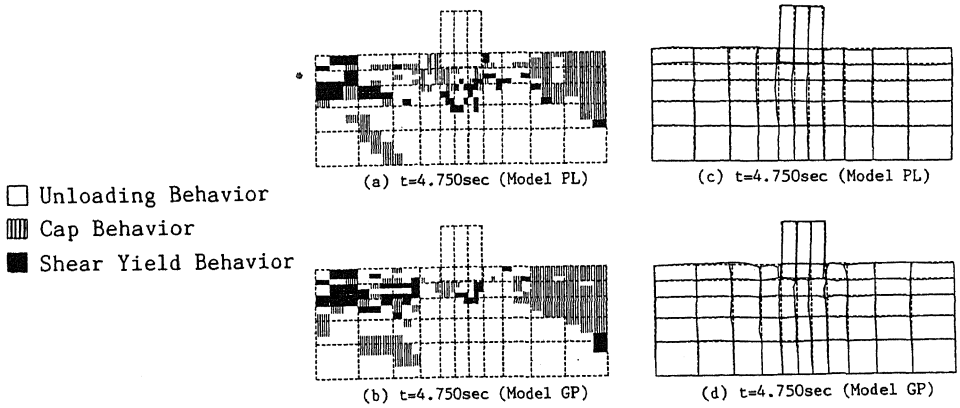

Fig.11 Overall Soil Behavior and Response Acceleration for Model PL and GP (Period of 0.5sec)

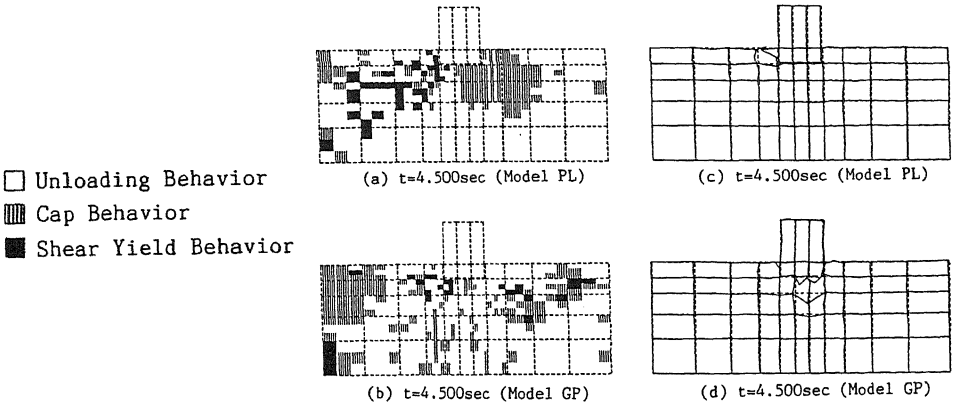

Fig.12 Overall Soil Behavior and Response Acceleration for Model PL and GP (Period of 1.0sec)

CONCLUSION

In this study theoretical analyses were performed by using the kinematic cap model for soil and by using finite element method. The dynamic response analyses for simple harmonic excitation were performed for four types of models.

As the results of this study, following behaviors of soil-structure systems under harmonic excitations are obtained. The responses at the top of the structure for four models are different from each other. High frequency component responses occur when material non-linearity for the soil and geometrical non-linearity between the soil and the structure are considered. Especially the effect of rebonding for higher frequency responses is clear, but the damping effects of soil plastification are also seen. Yielding region of the soil around the structure would be lessened by the introduction of geometrical non-linearity because overstimation of stress is prevented.

The soil beneath the structure and near the fixed boundary is comparatively stable due to the expansion of the cap model and enlarged elastic region by the loading from the structure. Progressive plastification process of the soil and the energy damping caused by two non-linearities depend on the periods of input waves.

It is concluded that in the dynamic response analysis of soil-structure systems, it is important to take into account of material non-linearity of the soil and geometrical non-linearity at the interface of the structure and the soil.

REFERENCES

1. Vaughan,D.K., Isenberg,J., Soil-Structure Interaction in Explosive Testing of Model Containments. North-Holland, Amsterdam, Nuclear Engineering and Design 77, pp.229-250, 1984
2. Isenberg,J, Vaughan,D.K., Sandler,I.S., Nonlinear Soil-Structure Interaction. Weidlinger Associates, Final Report to Electric Power Research Institute, EPRI NP-945, December 1978
3. Zaman,M.M., Desai,C.S., Drumm,E.C., Interface Model fof Dynamic Soil-Structure Interaction. Proc. ASCE, Vol.110, No.GT9, pp.1257-1273, 1984
4. Toki,K., Miura,H., Non-linear Seismic Response Analysis of Soil-Structure Interaction System. Proc. JSCE, No.317, pp.61-82, 1982-1
5. Tanaka,Y., Yashiro,H., Araki,H., Abe,T., Non-linear Seismic Response Analysis of Soil-Structure Interaction Systems. Summaries of Technical Papers of Annual Meeting, Architectural Institute of Japan, 1986
6. Tanaka,Y., Yashiro,H., Araki,H., Abe,T., Non-linear Seismic Response Analysis of Soil-Structure Interaction Systems with Separation and Sliding. Summaries of Technical Papers of Annual Meeting, Architectural Institute of Japan, No.2284, pp.567-568, 1987